THE YIELD OF $O_2(b\,^1\Sigma_g^+)$ IN OXYGEN ATOM RECOMBINATION†

E. A. OGRYZLO, Y. Q. SHEN and P. T. WASSELL
Department of Chemistry, University of British Columbia, Vancouver V6T 1Y6 (Canada)
(Received January 20, 1984; in revised form February 21, 1984)

Summary

The rate of formation of $O_2(b)$ when oxygen atoms recombine has been monitored in a fast flow system by following the emission at 762 nm as a function of time. The formation rate was found to be very sensitive to the amount of O_2 in the stream. A kinetic study of this process showed that it could be described by a mechanism in which the recombination of oxygen atoms in a termolecular reaction forms an unidentified precursor that is quenched principally by oxygen atoms and yields $O_2(b)$ through collisions with oxygen molecules. Several of the rate constants for the reactions involved have been determined at 300 K. The relevance of these results to the night airglow is discussed.

1. Introduction

The factors that control the yield of any electronically excited state formed by atom recombination remain to be established. It has been suggested that two such factors might be the relative degeneracies of the bound states and the shapes of the potential energy curves at large internuclear distances [1]. However, there is as yet no certainty that these factors are indeed important or that there are not other unidentified controlling factors. Consequently it remains important to establish experimentally the yields of such states during atom recombination.

For O_2 the determination of the yields of the various bound electronically excited states that correlate with $O(^3P)$ atoms is of practical significance because emission from all these states is observed in the night airglow [2, 3]. For example, an emission of about 6 kilorayleighs (kR) (corresponding to about 3.2×10^3 photons cm^{-3} s^{-1}) has been reported at 762 nm from $O_2(b)$. This emission has been reported to be centred at an altitude of 94 km [3] where $[O] = 5 \times 10^{11}$ atoms cm^{-3}, $[N_2] = 3 \times 10^{13}$ molecules cm^{-3}, $[O_2] = 5 \times 10^{12}$ molecules cm^{-3} and the total particle con-

†Paper presented at the COSMO 84 Conference on Singlet Molecular Oxygen, Clearwater Beach, FL, U.S.A., January 4 - 7, 1984.

0047-2670/84/$3.00

centration [M] = 3.5×10^{13} molecules cm^{-3}. Assuming that the emission is excited by the reactions

$$O + O + M \longrightarrow O_2(b) + M \quad (1)$$

$$O_2(b) + N_2 \longrightarrow O_2(a) + N_2 \quad (2)$$

$$O_2(b) \longrightarrow O_2(X) + h\nu \quad (3)$$

where $k_3 = 0.079\ s^{-1}$ [4] and $k_2 = 3 \times 10^{-15}\ cm^3\ molecule^{-1}\ s^{-1}$ [5] the emission intensity at 94 km should be given by

$$I(762\ nm) = \frac{k_1[O]^2[M]}{1 + (k_2/k_3)[N_2]}$$

It follows that a value of about $3 \times 10^{-33}\ cm^6\ molecule^{-2}\ s^{-1}$ is required for k_1 to account for the observed emission intensity. This corresponds to about 30% of the total recombination rate constant at 196 K [6].

A laboratory study of reaction (1) was undertaken by Young and coworkers [7, 8]. They determined a value of $1.7 \times 10^{-37}\ cm^6\ molecule^{-2}\ s^{-1}$ for k_1, which is more than four orders of magnitude smaller than the value required to explain the nightglow emission. However, one of their qualitative observations indicates that it may be possible to reconcile the laboratory and the atmospheric results. Young and Black [8] observed that when small amounts of O_2 were added to the gas stream containing only N_2 and oxygen atoms there was a sharp increase in the $O_2(b)$ produced. Their experiments were carried out in a bulb with a long residence time and it was consequently difficult to unravel the mechanism by which the O_2 affected the production rate. They did suggest, however, that their observations were consistent with the formation of a precursor in the recombination process, followed by conversion of this precursor to $O_2(b)$ in collisions with O_2. Young and Black suggested that the precursor might be $O_2(X, v = 9)$ or $O_2(a, v = 3)$.

More recently Witt *et al.* [9] showed that the direct recombination mechanism described by eqn. (1) could not be fitted to their night airglow measurements, whereas an indirect mechanism involving a precursor could be fitted to their data provided that about 80% of the recombining oxygen atoms form the precursor and almost every precursor that is quenched by O_2 produced $O_2(b)$.

In 1983 Kenner and Ogryzlo [10] reported that when O_2 is added to a stream of $O_2(c, v = 0)$ molecules, $O_2(b)$ is produced. Although they suggested that this lends support to the proposal of Witt *et al.* [9], it is worth observing that their system [10] also contained $O_2(A)$ and $O_2(A')$ molecules in vibrational levels up to $v' = 5$, which could also act as precursors for $O_2(b)$.

In the work described in this paper we have prepared oxygen atoms in an O_2-free fast flow system and have followed the appearance of $O_2(b)$ in an attempt to determine the mechanism and rate constants that govern its appearance.

2. Experimental procedure

The discharge flow system used to measure the formation of $O_2(b)$ is shown in Fig. 1. N_2 and NO in N_2 (9.81%) were obtained from Linde Speciality Gases and used directly from the cylinders. Further purification of these gases yielded the same results and was discontinued. N_2 was admitted to the flow system through a needle valve into a quartz tube (inside diameter, 10 mm) that was inserted into a 2.45 GHz discharge cavity. The NO–N_2 mixture was added through a titration inlet 3 cm above the main observation vessel (60 mm (inside diameter) × 70 cm). Oxygen (Matheson ultrahigh purity grade) could be added at various points along the tube through a movable multiple-jet inlet that facilitated rapid uniform mixing of the gases. The system was evacuated using two 500 l min^{-1} (at standard temperature and pressure) high vacuum pumps in parallel and flow rates of up to 2 m s^{-1} could be obtained in the main flow tube. A large orifice valve between the system and pumps was used to throttle the flow rate as required. Gas pressures in the system were measured using a Baratron capacitance manometer ((0 - 10) ± 0.001 Torr (absolute)).

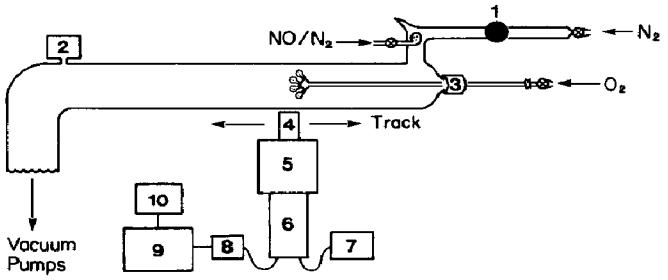

Fig. 1. Schematic diagram of the apparatus: 1, 2.45 GHz discharge cavity; 2, capacitance manometer; 3, variable inlet; 4, honeycomb collimator; 5, monochromator; 6, photomultiplier in cooled housing; 7, high voltage power supply; 8, preamplifier; 9, photon counter; 10, chart recorder.

The walls of the observation tube were coated with a thin film of halocarbon wax (Halocarbon Products Corporation series 12-00) to minimize heterogeneous atom recombination and deactivation of $O_2(b)$. This was done by washing the tube with a saturated solution of the wax in chloroform and allowing the solvent to evaporate. The discharge tube walls were poisoned with syrupy phosphoric acid to suppress atomic nitrogen recombination. Prior to the NO–N_2 titration inlet the partially dissociated gas was passed through a glass wool plug to remove vibrationally excited N_2 [11].

$O_2(b)$ was monitored along the flow tube by the $O_2(b) \rightarrow O_2(X)$ (0,0) emission at 762 nm. A blackened honeycomb collimator was fitted to the entrance slit of a 0.25 m Bausch and Lomb monochromator to limit its field of view to 1 cm of the horizontal axis in the centre of the main flow tube. A filter was used to eliminate lower order transmissions from the 1 μm blazed grating. The light was detected with an RCA C31034 (60 ER GaAs response)

photomultiplier tube housed in a thermoelectric cooled housing maintained at −20.0 °C. The output signal of the photomultiplier was conditioned by a preamplifier and fed to an Ortec photon counting system and then to a strip chart recorder.

The atomic oxygen was generated by adding NO to the atomic nitrogen stream until the "null point", where the concentration of atomic oxygen was equal to the amount of NO added.

The detector system was calibrated for the measurement of absolute intensities by observing the NO_2 continuum emission from known concentrations of NO and atomic oxygen [12]. The absolute emission rate constants reported by Sutoh *et al.* [13] were used in the calibration.

3. Results

3.1. Steady state measurements

Preliminary observations on the appearance of $O_2(b)$ in the stream of oxygen atoms confirmed earlier reports [7, 8] that indicated that the addition of small amounts of O_2 greatly enhanced the production of $O_2(b)$. However, the behaviour of the O_2-induced emission was not found to be consistent with a simple accelerated termolecular process described by reaction (1) with $M \equiv O_2$. Since the quenching of $O_2(b)$ by O_2 is less efficient than quenching by the principal bath gas (N_2), the removal of $O_2(b)$ is governed by reaction (2) and should remain constant as O_2 is added. A simple first-order dependence of the emission intensity on $[O_2]$ should therefore be observed. However, as shown in Fig. 2, the steady state concentration of $O_2(b)$ reaches a maximum with the addition of a relatively small amount of O_2. Such behaviour is inconsistent with the simple mechanism described by eqns. (1) and (2). However, the observation can be explained if the recombination of atoms produces a precursor (O_2^*) that is converted to $O_2(b)$ only in collisions with O_2. This mechanism, which also assumes that O_2^* is quenched principally by oxygen atoms in the absence of O_2, is described by reactions (2), (3) and the following:

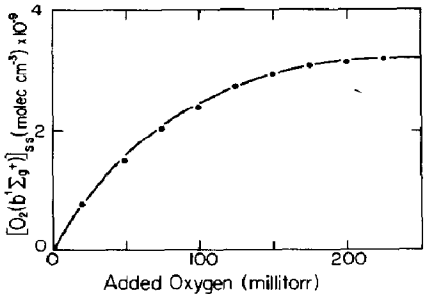

Fig. 2. $O_2(b\,^1\Sigma_g^+)$ concentration as a function of added O_2 ($[O] = 2.14 \times 10^{14}$ atoms cm^{-3}; $[N_2] = 6.62 \times 10^{16}$ molecules cm^{-3}).

$$O + O + M \longrightarrow O_2^* + M \quad (4)$$

$$O_2^* + O \longrightarrow \text{quenched products} \quad (5)$$

$$O_2^* + O_2 \longrightarrow \text{all products} \quad (6a)$$

$$O_2^* + O_2 \longrightarrow O_2(b) + O_2 \quad (6b)$$

where the rate constant for reaction (6b) is γk_6 and $\gamma = 1$ if the products of reactions (6a) and (6b) are the same. This mechanism predicts an $O_2(b)$ steady state concentration given by the following rate law:

$$[O_2(b)]_{ss} = \frac{\gamma k_4 k_6 [O]^2 [O_2][M]}{k_2[N_2](k_5[O] + k_6[O_2])} \quad (7)$$

If this energy transfer mechanism is correct, then when the O_2 concentration is large so that $k_6[O_2] \gg k_5[O]$ the rate law reduces to the form

$$[O_2(b)]_{ss} = \frac{\gamma k_4 [M]}{k_2[N_2]}[O]^2 \quad (8)$$

and, when the O_2 concentration is small, reduces to the form

$$[O_2(b)]_{ss} = \frac{\gamma k_4 k_6 [M]}{k_5 k_2 [N_2]}[O][O_2] \quad (9)$$

An experimental test of these predictions is contained in the measurements summarized in Figs. 3 and 4. Figure 3 shows that at high O_2 concentrations the emission from $O_2(b)$ is second order in [O], consistent with eqn. (8). In Fig. 4 the same type of plot yields a first-order dependence on [O] when $[O_2]$ is small, as predicted by eqn. (9).

The gradual change in the dependence of the $O_2(b)$ steady state concentration on $[O_2]$ from first order (as predicted by eqn. (9)) to zero order (as predicted by eqn. (8)) is illustrated by the curve in Fig. 2.

To extract rate constant ratios from these steady state experiments eqn. (7) was rearranged to the form

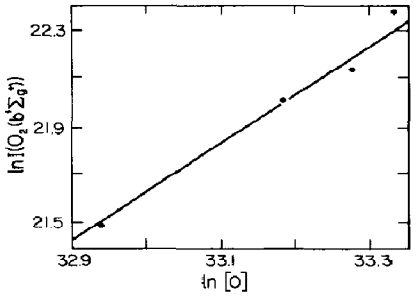

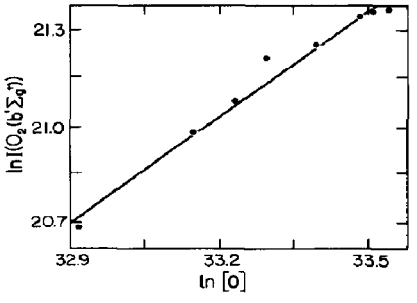

Fig. 3. A plot showing the second-order dependence of $[O_2(b^1\Sigma_g^+)]$ on atomic oxygen at relatively high concentrations of O_2 ($[O_2] = 6.24 \times 10^{15}$ molecules cm^{-3}): slope of line, 2.

Fig. 4. A plot showing the first-order dependence of $[O_2(b^1\Sigma_g^+)]$ on atomic oxygen at relatively small concentrations of O_2 ($[O_2] = 4.48 \times 10^{14}$ molecules cm^{-3}): slope of line, 1.

$$\frac{[O]^2[M]}{[O_2(b)][N_2]} = \frac{k_2}{\gamma k_4}\left(\frac{k_5[O]}{k_6[O_2]} + 1\right)$$

and the left-hand side was plotted against the ratio $[O]/[O_2]$ as shown in Fig. 5. (The data for Fig. 5 are given in Table 1.) The intercept and the ratio of the slope to the intercept of the line drawn through these points yield

$$\frac{\gamma k_4}{k_2} = (6.1 \pm 2.3) \times 10^{-20} \text{ cm}^3 \text{ molecule}^{-1}$$

and

$$\frac{k_5}{k_6} = 2.6 \pm 1.2$$

3.2. Rise time measurements

In the absence of added O_2 the $O_2(b)$ concentration at the first observation point was undetectably small when $(1 - 4) \times 10^{14}$ oxygen atoms cm^{-3} were allowed to flow into the observation tube. Under these conditions the $O_2(b)$ concentration slowly built up to a value of about 7×10^8 molecules cm^{-3} at the end of the observation tube. Measurements on this system are difficult to interpret because the O_2 concentration is slowly building up along the tube and this molecule greatly increases the $O_2(b)$ formation rate. When O_2 is added to the stream in the observation area there occurs a dramatic increase in the rate of formation of $O_2(b)$ as shown in Fig. 6. When excessive amounts of O_2 are added the $O_2(b)$ concentration passes through a maximum and then decreases towards the end of the tube. Under these conditions the oxygen atom concentration is found to be depleted by

$$O + O_2 + M \longrightarrow O_3 + M \qquad (10)$$

and all the "drop" of the $O_2(b)$ steady state concentration in this region can be accounted for by this loss of atoms together with a small contribution from

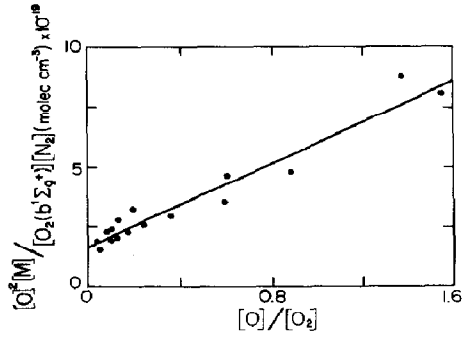

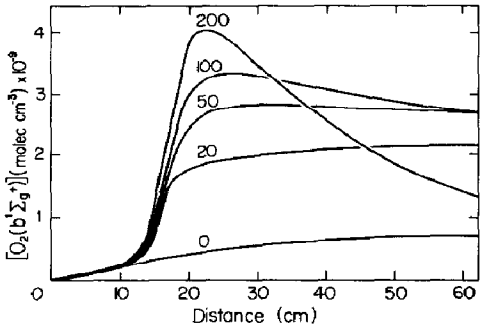

Fig. 5. Overall dependence of the $O_2(b^1\Sigma_g^+)$ concentration, corrected for [O], [M] and $[N_2]$, as a function of the $[O]/[O_2]$ ratio: slope, 4.3×10^{19} molecules cm^{-3}; intercept, 1.6×10^{19} molecules cm^{-3}.

Fig. 6. $[O_2(b^1\Sigma_g^+)]$ as a function of distance along the flow tube. The numbers on each curve show the amount of O_2 (mTorr) added at the 15 cm position.

TABLE 1

$[O_2] \times 10^{-14}$ (molecules cm^{-3})	$[O] \times 10^{-14}$ (atoms cm^{-3})	$[O_2(b)]_{ss} \times 10^{-9}$ (molecules cm^{-3})	$[N_2] \times 10^{-16}$ (molecules cm^{-3})	$[M] \times 10^{-16}$ (molecules cm^{-3})	$[O]^2[M]/[O_2(b)][N_2] \times 10^{-19}$ (molecules cm^{-3})	$[O]/[O_2]$
2.24	3.08	1.09	6.05	6.07	8.7	1.38
2.24	3.47	1.54	6.08	6.11	7.9	1.55
2.24	2.00	0.84	5.94	5.96	4.8	0.89
2.56	1.55	0.52	5.89	5.91	4.6	0.61
1.63	2.25	1.91	5.96	6.12	2.7	0.14
1.63	3.22	3.34	6.05	6.21	3.2	0.20
1.63	1.70	1.57	5.89	6.06	1.9	0.10
3.26	1.71	2.04	5.9	6.22	1.5	0.05
3.26	2.53	2.99	5.97	6.29	2.3	0.08
3.26	3.50	5.53	5.98	6.39	2.4	0.11
7.04	4.21	5.23	6.17	6.24	3.4	0.60
11.8	4.40	6.76	6.16	6.29	2.9	0.37
17.3	4.39	7.87	6.16	6.33	2.5	0.25
25.0	4.37	8.84	6.15	6.40	2.3	0.18
32.6	4.35	9.62	6.15	6.47	2.1	0.13
101	4.16	10.7	6.14	7.15	1.9	0.04

$$O_2(b) + O_3 \longrightarrow \text{quenched products} \quad (11)$$

To obtain rate constants for reactions (4) and (6), experiments were conducted at O_2 concentrations that are low enough to avoid depletion of atomic oxygen by reaction (10), but large enough to make reaction (4) rate controlling. Under these conditions the rise of the $O_2(b)$ concentration from the point of O_2 addition is illustrated in Fig. 7. It is not difficult to show that the rate at which $O_2(b)$ rises to the steady state concentration $[O_2(b)]_{ss}$ is given by

$$[O_2(b)]_{rel} = [O_2(b)]_{ss} \exp(-k_2[N_2]t) \quad (12)$$

where

$$[O_2(b)]_{rel} = [O_2(b)]_{ss} - [O_2(b)]_t \quad (13)$$

The quenching rate constant k_2 can therefore be obtained from the plot shown in Fig. 8. From the slope of this line

$$k_2 = 2.9 \times 10^{-15} \text{ cm}^3 \text{ molecule}^{-1} \text{ s}^{-1}$$

γk_4 can be calculated from the steady state concentration using the relationship

$$\gamma k_4 [O]_{ss}^2 [M] = k_2 [O_2(b)]_{ss} [N_2] \quad (14)$$

From the steady state limit in Fig. 8 we obtain

$$\gamma k_4 = 1.34 \times 10^{-34} \text{ cm}^6 \text{ molecule}^{-2} \text{ s}^{-1}$$

γk_4 can also be obtained by combining the above value of k_2 with the ratio

$$\frac{\gamma k_4}{k_2} = 6.1 \times 10^{-20} \text{ cm}^3 \text{ molecule}^{-1}$$

which was obtained in Section 3.1. This yields a value of

$$\gamma k_4 = 1.77 \times 10^{-34} \text{ cm}^6 \text{ molecule}^{-2} \text{ s}^{-1}$$

A weighted average of all our measurements yields a value of $\gamma k_4 = (1.6 \pm 0.6) \times 10^{-34} \text{ cm}^6 \text{ molecule}^{-2} \text{ s}^{-1}$.

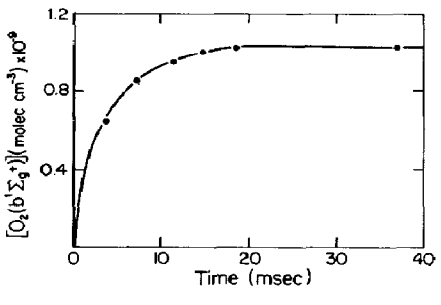

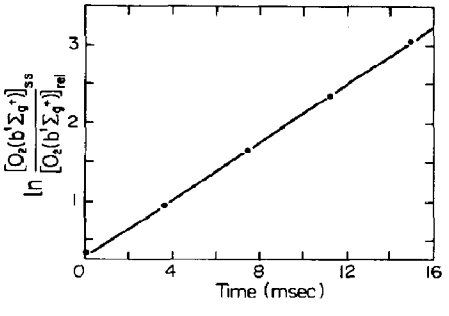

Fig. 7. The $[O_2(b^1\Sigma_g^+)]$ resulting from the addition of O_2 at $t = 0$ as a function of time.

Fig. 8. A linear plot based on eqn. (12). The data are taken from Fig. 7.

4. Discussion

The results presented in this paper confirm the earlier measurements that show that the direct formation of $O_2(b)$ in reaction (1) is a very inefficient reaction that could not account for the night airglow. The kinetic evidence is consistent with an excitation mechanism in which the recombination of oxygen atoms produces an excited state of O_2 (the "precursor") that is quenched by oxygen atoms and can yield $O_2(b)$ only in collisions with O_2. A quantitative analysis of our experimental data in terms of this mechanism yields an $O_2(b)$ quenching constant given by

$$k_2 = 2.9 \times 10^{-15} \text{ cm}^3 \text{ molecule}^{-1} \text{ s}^{-1}$$

that is consistent with earlier values [5]. A value of 1.6×10^{-34} for γk_4 means that if reaction (6) yields $O_2(b)$ with a quantum yield of unity

$$k_4 = 1.6 \times 10^{-34} \text{ cm}^6 \text{ molecule}^{-2} \text{ s}^{-1}$$

However, if γ is less than unity, k_4 is proportionately larger. It follows that if the total atomic oxygen recombination rate at room temperature is 4.8×10^{-33} cm^6 molecule^{-2} s^{-1} [6], the precursor is a state into which at least 3% of the recombination occurs.

Although it is not possible to determine the individual rate constants k_5 and k_6, the ratio

$$\frac{k_5}{k_6} = 2.6$$

that we obtained is potentially useful in the identification of the precursor O_2^*. Currently this ratio of rate constants has only been reported for $O_2(A^3\Sigma_u^+, v = 0 - 4)$ where $k_5/k_6 = 100$ [10] and $O_2(c^1\Sigma_u^-, v = 0)$ where $k_5/k_6 = 200$ [10]. It would therefore appear that none of these is an acceptable precursor for $O_2(b)$. However, it remains possible that higher vibrational levels of either of these states could be the precursor. The unobserved, but apparently weakly bound, $O_2(^5\Pi_g)$ state also remains a possibility [1].

If we attempt to apply our data to the night airglow several problems arise. Simple steady state analysis of the mechanism described by eqns. (2) - (6) yields

$$I(762 \text{ nm}) = \frac{\gamma k_4 [O]^2 [O_2][M]}{(k_5/k_6[O] + [O_2])(1 + k_2/k_3[N_2])} \tag{15}$$

where

$$\gamma k_4 = 1.6 \times 10^{-34} \text{ cm}^6 \text{ molecule}^{-2} \text{ s}^{-1}$$

$$\frac{k_5}{k_6} = 2.6$$

$$\frac{k_2}{k_3} = 3.7 \times 10^{-14} \text{ cm}^3 \text{ molecule}^{-1}$$

and the particle concentrations are those listed in Section 1 (*i.e.* at 94 km). Substitution of these values into eqn. (15) yields an emission intensity of 530 photons cm^{-3}, which is only about 16% of the observed emission.

There are several reasons why our constants might yield a small value for this intensity. Firstly, our values have been determined at 300 K. The temperature at 94 km is closer to 190 K. In view of the increase in the total recombination rate constant with decreasing temperature [6] it is quite possible that k_4 is larger at lower temperatures. Secondly, our experiments are conducted at pressures that are almost four orders of magnitude higher than those that occur near 94 km. In view of the fact that O_2^* is most probably electronically excited oxygen with an unrelaxed vibrational distribution, it is likely to have a much higher vibrational temperature in the upper atmosphere where fewer collisions occur. Consequently a more efficient production of $O_2(b)$ from the precursor is not unreasonable.

References

1 P. C. Wraight, *Planet. Space Sci., 30* (1982) 251.
2 T. C. Slanger and D. L. Heustis, *J. Geophys. Res., 86* (1981) 3551.
3 R. G. H. Greer, E. J. Llewellyn, B. H. Solheim and G. Witt, *Planet. Space Sci., 29* (1981) 383.
4 A. J. Deans, G. G. Shephard and W. F. J. Evans, *J. Geophys. Res. Lett., 3* (1976) 441.
5 R. J. O'Brien, Jr., and G. H. Myers, *J. Chem. Phys., 53* (1970) 3832.
6 I. M. Campbell and C. N. Gray, *Chem. Phys. Lett., 18* (1973) 604.
7 R. A. Young and R. L. Sharpless, *J. Chem. Phys., 39* (1963) 1071.
8 R. A. Young and G. Black, *J. Chem. Phys., 44* (1966) 3741.
9 G. Witt, J. Stegman, B. Solheim and E. J. Llewellyn, *Planet. Space Sci., 27* (1979) 341.
10 R. D. Kenner and E. A. Ogryzlo, *Can. J. Chem., 61* (1983) 921.
11 J. E. Morgan, L. F. Phillips and H. I. Schiff, *Discuss. Faraday Soc., 33* (1962) 118.
12 A. Fontijn, C. B. Meyer and H. I. Schiff, *J. Chem. Phys., 40* (1964) 46.
13 M. Sutoh, M. Morioka and M. Nakamura, *J. Chem. Phys., 72* (1980) 1.